KI REPORTS
KIReports.org
TRANSLATIONAL RESEARCH

Glomerulopathic Light Chain-Mesangial Cell Interactions: Sortilin-Related Receptor (SORL1) and Signaling

Guillermo A. Herrera[1,2], Luis del Pozo-Yauner[1], Jiamin Teng[1], Chun Zeng[1], Xinggui Shen[4], Takahito Moriyama[5], Veronica Ramirez Alcantara[3], Bing Liu[1] and Elba A. Turbat-Herrera[1,3]

[1]Department of Pathology, College of Medicine, University of South Alabama, Mobile, Alabama, USA; [2]Department of Physiology and Cell Biology, College of Medicine, University of South Alabama, Mobile, Alabama, USA; [3]Mitchell Cancer Institute, College of Medicine, University of South Alabama, Mobile, Alabama, USA; [4]Louisiana State University, Health Sciences Center, Shreveport, Louisiana, USA; and [5]Department of Medicine, Kidney Center, Tokyo Women's Medical University, Tokyo, Japan

Introduction: Deciphering the intricacies of the interactions of glomerulopathic Ig light chains with mesangial cells is key to delineate signaling events responsible for the mesangial pathologic alterations that ensue.

Methods: Human mesangial cells, caveolin 1 (CAV1), wild type (WT) ,and knockout (KO), were incubated with glomerulopathic light chains purified from the urine of patients with light chain–associated (AL) amyloidosis or light chain deposition disease. Associated signaling events induced by surface interactions of glomerulopathic light chains with caveolins and other membrane proteins, as well as the effect of epigallocatechin-3-gallate (EGCG) on the capacity of mesangial cells to intracellularly process AL light chains were investigated using a variety of techniques, including chemical crosslinking with mass spectroscopy, immunofluorescence, and ultrastructural immunolabeling.

Results: Crosslinking experiments provide evidence suggesting that sortilin-related receptor (SORL1), a transmembrane sorting receptor that regulates cellular trafficking of proteins, is a component of the receptor on mesangial cells for glomerulopathic light chains. Colocalization of glomerulopathic light chains with SORL1 in caveolae and also in lysosomes when light chain internalization occurred, was documented using double immunofluorescence and immunogold labeling ultrastructural techniques. It was found that EGCG directly blocks c-Fos cytoplasmic to nuclei signal translocation after interactions of AL light chains with mesangial cells, resulting in a decrease in amyloid formation.

Conclusion: Our findings document for the first time a role for SORL1 linked to glomerular pathology and signaling events that take place when certain monoclonal light chains interact with mesangial cells. This finding may lead to novel therapies for treating renal injury caused by glomerulopathic light chains.

Kidney Int Rep (2021) **6,** 1379–1396; https://doi.org/10.1016/j.ekir.2021.02.014
KEYWORDS: AL-amyloidosis; caveolins; immunoglobulin light chains; light chain deposition disease; mesangial cell; receptor; SORL1

Most of the Ig light chains (LCs) circulate in the bloodstream covalently linked to the heavy chain, as part of antibodies. However, under physiological conditions, plasma cells produce 30% to 40% excess of LCs, the excess being secreted into the bloodstream in free state (fLCs).[1–3] Despite the relatively large fraction of LCs that reaches the vascular compartment as fLCs, their concentration in the serum of healthy individuals is approximately 1000-fold lower than that of the Ig-bound LCs.[1] This is because fLCs are quickly cleared from the blood, with a half-life of 2 to 6 hours,[4] significantly shorter than the half-life of 20 to 25 days of the intact IgG.[1] The kidneys are where most of the fLCs are catabolized.[5] Like other low molecular weight proteins,[6] fLCs are filtered in the glomerulus and reach the proximal tubules, where they are readily reabsorbed by proximal tubular cells.[1] Two large membrane glycoproteins, megalin (600 kDa) and cubilin (460 kD), work in tandem to mediate the endocytosis of fLCs by the tubular cells.[7,8] These protein receptors are strongly expressed in the brush border of proximal tubular cells and are responsible for the endocytosis of low molecular weight proteins, such as LCs, but also of some nutrients, such as vitamins and some

Correspondence: Guillermo A. Herrera, Department of Pathology, University of South Alabama, College of Medicine, 2451 USA Medical Center Drive, Mobile, Alabama 36617, USA. E-mail: gherrera@health.southalabama.edu

Received 21 January 2021; accepted 8 February 2021; published online 13 March 2021

oligo elements.[9] Once endocytosed, polyclonal fLCs are routed to the lysosomal compartment, where they are degraded into short peptides and free amino acids, which are then recycled. In addition to the normal polyclonal fLCs, the megalin-cubilin tandem endocytic receptor also mediates the uptake of monoclonal fLCs that are overproduced in patients with monoclonal gammopathies, such as multiple myeloma.[8,10] Approximately 85% of the monoclonal fLCs are nephrotoxic. Of them, approximately 70% cause tubular damage and are referred to as tubulopathic LCs (TLCs).[11,12] The remaining 30% interact with the glomerular mesangium and triggers pathogenic events that result in glomerular damage. This group of LCs are named glomerulopathic LCs (GLCs) and, depending on their structural and physicochemical properties, can produce 2 main diseases: (1) LC deposition disease (LCDD) and LC-derived (AL) amyloidosis.[13,14] Previous studies have demonstrated that the potential of the GLCs to elicit damage is related to their ability to interact with membranes of mesangial cells (MCs).[11,15–18]

Existing data indicate that both types of GLCs, LCDD- and AL-LCs, compete for the same receptor through a saturable mechanism.[16,18] Although mediated by the same membrane receptor, the interactions of LCDD or AL-derived LCs with MCs lead to divergent downstream MCs/extracellular matrix alterations resulting in diametrically opposite changes in mesangial homeostasis.[16,17,19–22] In the case of LCDD-LCs, the interaction with the membrane receptor induces the transformation of MCs from their normal smooth muscle phenotype to a myofibroblastic type, with the acquisition of increased rough endoplasmic reticulum to endow these with the required organelles for increased protein production (mostly tenascin).[17] It is important to mention that such alterations do not follow the internalization of the LCDD-LC.[19] In contrast, the interaction of AL-LCs with the MCs triggers LC internalization and eventual transport to the mature lysosomal compartment, where amyloid fibril formation occurs.[17] This phenomenon is accompanied by the conversion of MCs to a macrophage phenotype to acquire the ability to endocytose the LCs and eventually deliver them to the mature lysosomal compartment,[17] using Rab proteins for the intracellular transport of the LCs.[18] Studies have shown that phenotypic cellular changes are mediated through activation of c-Fos in both situations.[16]

Because cubilin and megalin are not present on MCs,[18] it can be inferred that a different membrane receptor is the target of the GLCs. In this study, sortilin-related receptor, also known as SORLA, a protein encoded by *SORL1* gene, is found to be involved in the mechanism of internalization of the GLCs in MCs. It is also shown that activation of caveolins is part of the signaling mechanism initiated at the MC membranes by the interaction with GLCs. Finally, it is documented that the activation of nuclear factor (NF)-κB and c-Fos signaling pathways that results from the interaction of GLCs with the MCs, can be modulated by treatment of the cells with EGCG bypassing CAV1. Taken together, our data suggest potential new therapeutic strategies for dealing with the renal damage in LCDD and AL-amyloidosis.

MATERIALS AND METHODS

Isolation, Purification, and Characterization of LCs

GLCs were obtained from the urine of patients with renal biopsy-documented AL-Am (n = 3) and LCDD (n = 3). TLCs obtained from the urine of patients with myeloma (cast) nephropathy (n = 2) and proximal tubulopathy (n = 1) were used as controls. The fLCs were purified from the urine following a well-characterized protocol established in our laboratory and described in detail elsewhere.[23] Briefly, the fLCs were precipitated from the urine adding ammonium sulfate up to 70% of saturation and sedimented by centrifugation at 3400 g at 4°C for 30 minutes. The pellet was dissolved in distilled water and dialyzed for at least 24 hours using cellulose dialysis tubing with a 12,000 to 14,000 Da cutoff (Spectrum Spectra Membrane Tubing; Fisher Scientific, Pittsburgh, PA). A second step of dialysis was performed in 0.01 M sodium phosphate buffer, pH 7.6, for 24 hours. The dialyzed solution was then centrifuged at 7500 g at 4°C for 30 minutes to get rid of debris. The supernatant was filtered through a 0.22-μm pore size membrane to eliminate the persistent aggregates. The filtered protein solution was fractionated by ultrafiltration in a centrifugal concentrator with a 300-kDa molecular weight cutoff membrane (Pall Life Sciences, Port Washington, NY). The filtered solution was then concentrated in a centrifugal concentrator with a 3-kDa molecular weight cutoff membrane, dialyzed using a 3.5 kDa molecular weight cutoff membrane dialysis tube and analyzed by sodium dodecyl sulfate-polyacrylamide gel electrophoresis (SDS-PAGE) to evaluate the purity of the LC preparation. Purified LCs were further analyzed by zone electrophoresis on agarose gel in 50 mmol/l barbital buffer, pH 8.6 and immunotyped by immunofixation using anti-κ or -λ polyclonal antibodies, following the manufacturer's recommendation. The concentration of the LC stock solutions was determined using the Pierce BCA Protein Assay kit (Thermo

Scientific, Rockford, IL) following the manufacturer's recommendations. LC stocks at 2 mg/ml were prepared and supplemented with a penicillin-streptomycin solution (100×; Sigma-Aldrich, St Louis, MO) to avoid bacterial growth. LC solutions were concentrated, dialyzed against 0.9% NaCl, filtered through a sterile 0.2-μm filter membrane, aliquoted, and stored aseptically in sealed vials at 4°C until analysis. The LCs used for the various experiments were not pooled or combined in any manner.

Culture of Human Mesangial Cells

Human mesangial cells (HMCs) were isolated using the protocol initially described by Harper *et al.*[24] The cortexes of human kidneys surgically removed (from nephrectomies performed for malignancies) from areas away from the neoplasms were used. HMCs were isolated by sieving the cortex through stainless steel screens and a series of different pore size nylon sieves. HMCs were cultured in RPMI 1640 medium (Fisher Scientific, Suwanee, GA), supplemented with 20% fetal bovine serum at 37°C in a humidified atmosphere with 5% CO_2 and treated with a penicillin (100 U/ml)/streptomycin (100 μg/ml) solution (Sigma-Aldrich). HMCs overgrew other cells and became confluent 3 to 4 weeks after plating. In addition, HMCs were purchased from Fisher Scientific and maintained in culture conditions similar to described previously. For both HMC cultures, a homogeneous population of MCs was confirmed by ultrastructural examination showing smooth muscle features with intracytoplasmic myofilaments and attachment plaques at the cell surfaces, as well as immunohistochemical staining showing positivity for HHF-35 (muscle-specific antigen) and vimentin and lack of staining for keratins and factor VIII. On reaching confluence, cells were seeded into 100-mm tissue culture dishes. Fifth to sixth passages of MCs were used for the experiments. The MCs were grown on RPMI 1640 medium containing 15% fetal bovine serum until confluence. Three days before the beginning of the experiments, the fetal bovine serum concentration of the media was decreased to 0.5% with daily exchange of medium to create a quiescent cellular environment prior to the incubation with LCs.

CAV1−/− Mice MC Preparation

CAV1 KO mice (CAV1−/− mice, CAV1 KO, CAV1tm1Mls/J) and CAV1+/+ mice (B6129PF2/J), were purchased from Jackson Laboratory (Bar Harbor, ME). These mice were of a mixed genetic background (129SV and c57 black 6), male, and aged 8 to 10 weeks. The kidneys were excised and washed with 70% alcohol to remove possible contamination. The kidney cortices were cut away from the medullae and chopped into millimeter-square pieces and passed through a series of steel sieves (W.S. Tyler, Inc, Mentor, OH) with decreasing pore sizes of 200 μ-pore (60 mesh, 2 mesh), 150 μ-pore (150 mesh, 7 mesh), 75 μ-pore (200 mesh, 36 mesh), with the glomeruli ending up on top of the 200-mesh sieve. Each step was rinsed with Hank's balanced salt solution. The tiny white dots representing glomeruli were collected. Then, the isolated glomeruli were rinsed twice in Hank's balanced salt solution, buffered with HEPES, pH 7.4 (HBSS), containing antibiotics (penicillin 100 U/ml, streptomycin, 100 μg/ml, and amphotericin, 0.25 μg/ml), and incubated with trypsin (0.2%) for 20 minutes at 37°C, followed by an incubation with 0.1% collagenase (189 U/ml; Worthington Diagnostics Systems, Inc., Lakewood, NJ) for 40 minutes at 37°C. After the specimen was washed once in buffered Hank's balanced salt solution and antibiotics, the pellet was then resuspended in RPMI 1640 media, and plated under the appropriated conditions to permit proliferation of the MCs.

Crosslinking of GLCs to MCs

Confluent monolayers of quiescent HMCs in 100-mm dishes were incubated for 30 minutes at room temperature with 10 μg/ml GLCs added to RPMI 1640 medium, pH 5.0, and containing 0.5% fetal bovine serum and 10 mM acetic acid. The medium was acidified to inhibit clathrin-mediated internalization of the LCs (primarily the AL-LCs). Afterward, cells were quickly rinsed twice with borate-buffered saline (10 mM $Na_2B_4O_7$, 150 mM NaCl, pH = 8) and incubated at room temperature with 1 mM 3,3′-dithiobis(sulfosuccinimidylpropionate) (DTSSP; Thermo Fisher Scientific, Colorado Springs, CO), a water-soluble membrane impermeable thio cleavage cross-linker. After 30 minutes, the crosslinking reaction was stopped by rinsing the cells 4 times with 20 mM Tris-buffered saline (TBS). These cells were then scraped from the dishes, pelleted by centrifugation at 1000 rpm (210*g*) for 5 minutes and lysed in 500 μl of a modified Laemmli buffer, 1× NuPAGE sample buffer (Invitrogen, Carlsbad, CA). The lysate was then centrifuged at 10,000*g* for 10 minutes at 4°C. Proteins contained within the lysate were resolved by SDS-PAGE under nonreducing conditions on NuPAGE 4% to 12%, Bis-Tris polyacrylamide gels using NuPAGE MOPS (3-[N-morpholino] propanesulfonic acid) SDS running buffer (Invitrogen). The resolved bands were transferred onto a polyvinylidene fluoride membrane (Millipore-Sigma, Burlington, MA). The membrane was blocked with 5% fat-free milk protein in TBS and immunodetection of the cross-linked protein complex containing LC was performed with rabbit anti-human κ or λ LC antibodies (primary antibodies) diluted 1:2000 (Abcam,

Cambridge, MA). Donkey anti-rabbit horseradish peroxidase-conjugated antibody diluted 1:1500 was used as secondary antibody and protein bands were detected using enhanced chemiluminescence reagent-ECL (Pharmacia, Uppsala, Sweden). SDS-PAGE gels were stained with Coomassie blue to allow the selection of shifted bands above 70 kDa to be analyzed by liquid chromatography (LC)-mass spectroscopy (MS), described as follows.

Gel Digestion and LC-MS Analysis

The LC gel bands were subjected to digestion using trypsin MS grade (Promega Corporation, Madison, WI). Tryptic peptides were analyzed by LC-MS using a NanoAcquity UPLC-Synapt High-definition mass spectrometer (Waters Corporation, Milford, MA). The nano-LC separation was performed using a BEH C18 reversed phase column (1.7 μm, 75 μm ID × 100 mm [Waters Corporation]). The binary solvent system used comprised 99.9% water and 0.1% formic acid (mobile phase A) and 99.9% acetonitrile and 0.1% formic acid (mobile phase B). Tryptic peptides were eluted at a flow rate of 0.4 μl/min using a gradient of 12% to 55% of solvent B for 120 minutes, then were introduced into the MS via nano-electrospray ionization source using a fused silica PicoTip emitter (10 μm tip diameter). MS analysis was performed in a positive ion mode (V mode), source temperature 100°C, capillary voltage 3.5 kV, sampling cone voltage 40 V, and extraction cone voltage of 2.0 V. Data were acquired using MassLynxTM 4.1 software (Waters Corporation) in an automatic data-dependent acquisition mode. MS–time of flight scans were acquired from m/z 300 to m/z 1500, and up to 3 precursor ions were selected for subsequent MS/MS scans from m/z 100 to 1500 using charge state recognition promote fragmentation. These proteins were identified by PEAKs Studio 7.5 (Bioinformatics Solutions Inc., Ontario, Canada), and then subjected to protein analysis through PANTHER version 14.0 and STRING version 10.0.

Colocalization Studies Using Indirect Immunofluorescence for κ and λ LCs and SORL1

HMCs on coverslips incubated with GLCs or control LCs were fixed in ice-cold methanol for 10 minutes at room temperature followed by incubation in phosphate-buffered saline (PBS) containing 0.25% Triton X-100 (PBS-T) for 10 minutes and washed in PBS 3 times for 5 minutes. Cells were then incubated with 1% of IgG- and protease-free bovine serum albumin (BSA) diluted in PBS for 30 minutes to block nonspecific binding of the antibodies. After incubation, cells were incubated with a mixture of primary antibodies: Texas red-labeled antibody directed to κ or λ LCs (Abcam) at a 1/100 dilution and a fluorescein-labeled anti-SORLA extracellular luminal domain mouse monoclonal antibody (clone 20C11, catalog number MABN1793; Sigma-Aldrich) diluted 1/1000 in 1% BSA in PBS-T in a humidified chamber for 1 hour at room temperature or overnight at 4°C. Then, the slides were incubated with a mixture of 2 secondary antibodies: goat anti-mouse Alexa Fluor 488 with goat anti-rabbit Alexa Fluor 594 antibody, both at 1 μg/ml, in 1% BSA for 1 hour at room temperature in the dark. Cells were then washed and incubated with 1 μg/ml DAPI (4′,6 diamine-2′-phenylindole dihydrochloride [Sigma-Aldrich]) for 1 minute to visualize the nuclei of the cells. Finally, cells were washed, mounted, and examined with a BH40 light microscope with fluorescence capabilities (Olympus Co, Center Valley, PA).

Transmission Electron Microscopy

MCs obtained from renal cortices were cultured on Matrigel matrix (Corning, Life Sciences, Arlington Heights, IL), a solubilized basement membrane preparation rich in collagen IV of similar composition to mesangial matrix and incubated with monoclonal LCs obtained from the urine of patients as described earlier. Specimens were cut into 1-mm cubes and fixed for at least 2 hours in glutaraldehyde (Ted Pella, Redding, CA) at room temperature. The preparations were then rinsed 3 times for 5 minutes each in an appropriate buffer, and post-fixed for 1 hour in 1% osmium tetroxide in distilled water. The samples were again rinsed 3 times for 5 minutes each in distilled water and then rehydrated in 50%, 70%, and 80% ethanol for 10 minutes, followed by rehydration in 95% ethanol with 2 changes within 10 minutes and 100% ethanol from a newly opened bottle for 3 changes within 15 minutes. The specimens were then placed in propylene oxide for 10 minutes, followed by a 1:1 solution of propylene oxide\resin for minimum of 1 hour, and a 1:2 propylene oxide/resin from 1 hour to overnight on a rotator. The tissues were embedded in 100% Epon resin (Polysciences Corporation, Warrington, PA) with 2 changes over 2 to 6 hours. Thick sections were cut, placed on slides, and stained with toluidine blue for survey. Using light microscopy, specific areas were selected, and thin sections were prepared. The thin sections stained with uranyl acetate and lead citrate were examined with a JEOL 1400 transmission electron microscope (Peabody, MA). Digitized images were obtained using a BioSprint12 (12 megapixel) charge-coupled device cameras (Advanced Microscopy Techniques, Scientex, Woburn, MA) and analyzed visually.

Ultrastructural Immunogold Labeling for κ/λ LCs, and SORL1 to Assess for Colocalization

Ultrastructural immunogold labeling for κ and λ LCs was performed following a method originally described by Herrera and Lott.[25] Briefly, thin sections obtained from HMC cultures incubated with LCs, were fixed in 10% formaldehyde for 24 hours, and embedded in Epon resin for electron microscopy. Embedded sections were placed on 200- to 300-mesh coated nickel grids and incubated with a 1:30 dilution of normal goat serum in 50 mM Tris buffer, pH 7.6 for 30 minutes at room temperature. Etching was performed using potassium permanganate. The sections were subsequently incubated with prediluted polyclonal rabbit antibodies (Abcam, Cambridge, UK) to κ (1/500 dilution) or λ (1/1000 dilution) LCs, and clone 20C11 mouse monoclonal anti-SorLA/SORL1 antibody (catalog number MABN1793, Sigma-Aldrich) at a 1/1000 dilution, in the case of colocalization studies. The grids were washed in TBS for 20 minutes and then in TBS containing 1% BSA for 10 minutes. Later, the grids were incubated for 1 hour at room temperature with a goat anti-rabbit IgG antibody (Abcam) labeled with 5 to 6 nm in diameter gold particles and a goat anti-mouse IgG antibody labeled with 15 to 16 nm in diameter gold spheres, in both cases diluted 1/15 in 20 mM TBS, pH 8.2, containing 1% BSA (Janssen Pharmaceuticals, Beerse, Belgium, distributed by Amersham, Life Science, Arlington Heights, IL). After several washes, grids were post-stained with uranyl acetate and lead acetate and examined using a transmission electron microscope (JEOL 1400). A renal biopsy showing diffuse proliferative lupus nephritis, characterized by abundant electron dense deposits and a "full-house" immunofluorescence staining pattern, served as the positive control. A renal biopsy showing minimal change disease with a negative "full-panel" of immunofluorescence stains and no immune complexes served as the negative control.

Comparison of Amyloid Formation When KO and WT CAV1 MCs Are Incubated With Amyloidogenic LCs

Both WT and CAV1 KO MCs were incubated with AL-LCs and TLCs for up to 72 hours to test for the effect of lack of CAV1, if any, on amyloid formation. Extracellular amyloid deposits per square area were quantitated and compared.

Effect of EGCG on the Interactions of GLCs and MCs

MCs were incubated with AL or TLCs for up to 72 hours and compared with the same MCs preceded by application of EGCG (dose determined as indicated later in this article) to test effect, if any, on amyloid formation.

Lactic Dehydrogenase Assay

To evaluate the concentration-dependent biological activity of EGCG in cultured cells, quiescent confluent cultures of MCs were incubated with low serum RPMI with different concentrations of ECGC (0, 5, 20, 50, and 100 μM) for 48 hours. After treatment, 50 μl of supernatant from each well was transferred to a separate 96-well titer plate for lactic dehydrogenase (LDH) colorimetric determination. Briefly, 50 μl of LDH solution (Promega Corporation) was added to each well and incubated in dark for 30 minutes at room temperature, followed by the addition of 50 μl of Stop Solution to each well. The LDH content was measured on a microplate reader at 490 nm. The amount of LDH released into the culture supernatant was calculated using a standard curve as reference.

Cell Proliferation Assay

To determine the effect of EGCG in cell proliferation, the number of MCs per well was assessed in the same culture plates from the LDH assay. Briefly, after removing 50 μl of serum free medium, 20 μl of a 1-step assay solution (CellTiter 96 AQueous One Solution Cell Proliferation Assay [MTS]; Promega) containing a tetrazolium compound was added to each well. The tetrazolium compound was bio-reduced by viable cells to colored formazan product that is soluble in culture medium. After a 60-minute incubation at 37°C and a cool down period, colorimetric determination of cell proliferation was determined using a plate reader at 490 nm. The number of viable cells was calculated using a standard curve. Data were expressed as mean ± SD.

Western Blots

To determine the effect of EGCG in the expression of NF-κB and c-Fos in MCs, quiescent, confluent monolayers of MCs grown on 150-mm culture dishes were incubated with GLCs at 10 μg/ml in the absence and presence of EGCG at different concentrations (0, 5, 20, 50, and 100 μM) for 48 hours. After treatment, cells were washed with sterile cold PBS pH 7.4. Cells were scraped, collected, and centrifuged at 4°C to collect pellet. After centrifugation, the supernatant was discarded, and pellet was washed twice by adding 1 ml of cold hypotonic phosphate buffer and centrifuged at 4°C. Then, cell pellets were resuspended on 1 ml of hypotonic phosphate buffer on ice and incubated for 20 minutes, and 7 μl of 10% NP-40 was added to lysate the cells incubating on ice for 5 minutes. Cell lysates were transferred to a 2-ml glass pestle and homogenized on ice by applying 10 gentle strokes of the pestle;

120 μl of the lysate was taken out and stored, representing the total protein sample. The rest of the lysate was centrifuged at 12,298 g at 4°C for 30 minutes, and the supernatant, representing the cytoplasmic fraction, was stored until analysis; 100 μl of low-salt buffer and 50 μl of hypertonic phosphate buffer were added to the pellet and gently rocked at 4°C overnight. After centrifugation at 10,000 rpm at 4°C, the supernatant, representing the nuclear fraction, was stored until analysis. Cytosolic and nuclear fractions were heated at 70°C in the presence of SDS-PAGE loading buffer for 10 minutes before being electrophoresed on 3.8% SDS-PAGE using NuPAGE MOPS SDS running buffer (Invitrogen). Protein bands were blotted onto polyvinylidene fluoride membranes using a transfer buffer containing 25 mM Tris, 192 mM glycine, and 20% methanol (pH 8.3). The membranes were blocked by overnight incubation at 4°C in 5% nonfat dry milk. The membranes were then washed 3 times and subsequently incubated overnight at 4°C with the primary rabbit antibodies against NF-κB p65 (Santa Cruz Biotechnology Inc, Dallas, TX) and c-Fos (Abcam), both at 1/200 dilution. The membranes were then washed 3 times with TBS containing 0.05% Tween (TTBS) at room temperature for 10 minutes with agitation and incubated with donkey anti-rabbit horseradish peroxidase (HRP)-conjugated secondary antibody (Amersham Biosciences, Buckinghamshire, UK) diluted at 1:1500. Membranes were washed 4 times with TBST at room temperature for 30 minutes with strong agitation. Bands were visualized by addition of Immun-Star HRP peroxide buffer and luminol/enhancer (Bio-Rad Laboratories, Irvine, CA). β actin (Sigma-Aldrich) diluted to 1:500 served as loading control for cytoplasm fraction and Lamin B1 (Abcam) diluted to 0.5 μg/ml as loading control for nuclear fraction. The effect of EGCG on NF-κB and c-Fos expression in WT and CAV1 KO MCs incubated with LCDD and AL-LCs was also analyzed following the described Western blot protocol.

Immunofluorescence Microscopy

Cellular localization of NF-κB and c-Fos protein expression was also analyzed using immunofluorescence microscopy. Briefly, MCs grown on coverslips were incubated with each GLCs and non-GLCs at 10 μg/ml and EGCG at 50 μM for 1 hour at room temperature. Cells were fixed in 3.7% formaldehyde in PBS pH 7.4 for 20 minutes. Permeability was performed with 100% methanol at −20°C for 15 minutes. After incubation with TTBS containing 3% BSA for 30 minutes, cells were incubated for 1 hour with anti-NF-κB p65 (Santa Cruz Biotechnology Inc, Dallas, TX) or c-Fos (Abcam, Cambridge, UK) rabbit antibody (primary antibody), both diluted 1/100 with TTBS containing 1% BSA, and then washed 3 times with TTBS for 5 minutes. Following, cells were incubated with secondary antibody Alexa Fluor 488-conjugated goat anti-rabbit IgG-H and L components (Molecular Probes, Eugene, OR) for 1 hour, and washed 3 times with TTBS for 5 minutes. A confocal fluorescence microscope (Nikon inverted Eclipse TE 300, Bio-Rad Radiance 2000 Laser Scanning Microscope) was used to observe the findings, and a Laser Sharp 2000 (Bio-Rad House, Hertfordshire, UK) software was used to capture the images. Extracellular amyloid deposits per square area were quantitated and the effect of EGCG on the ability of the different LCs to form amyloid inside the MCs was evaluated.

CAV1 Fluorescence Staining in MCs Incubated With and Without LCs

MCs on coverslips were incubated with AL or LCDD-LCs, or without LCs, for 30 minutes and then stained for CAV1 with a Texas Red-conjugated polyclonal antibody at 1:30 dilution (Santa Cruz Biotechnology, Santa Cruz, CA), using a direct fluorescence technique and compared.

Statistical Analysis

Data were expressed as mean ± SD. The unpaired *t*-test was used to compare LDH content and numbers of HMCs. Significance was considered as $P < 0.05$.

RESULTS

SORL1 Is Expressed When GLCs Are Incubated With MCs

Bands of different molecular weight were detected when GLCs interacted with MCs compared with when no LCs were placed to interact with MCs. Bands consisting in free (not cross-linked) LCs were also detected in the gels, resulting from the small number of LCs remaining unattached to MCs.

In 10 different experiments, more than 80 different proteins were detected by MS analysis, with approximately 15 to 20 of these proteins with receptor recognition in the different runs. MS data demonstrated that SORL1 (238 and 500 kDa) was the one unique membrane receptor expressed when 5 of the 6 GLCs but not when TLCs were incubated with MCs or when MCs by themselves (without LCs) were tested (Table 1).

Several transient MC receptors were shared by all 6 GLCs, including G-protein-coupled (caveolin signaling), ligand-gated ion channel/transient potential cation channel, subfamily M (calcium ion channel receptor), tyrosine-protein phosphatase (signal transduction), and extracellular matrix linker protein receptor/cell adhesion-molecule extracellular matrix glycoprotein receptors (Table 1). SORL1 expression

Table 1. Mass spectroscopy analysis to identify membrane proteins of MCs that were covalently linked to GLCs in the crosslinking experiments after 30 minutes of incubation of MCs with AL- or LCDD-LC

	Control			GLC					
	Non-DSTTP	No LC	TLC	AL1-λ	AL2-λ	AL3-λ	LCDD1-κ	LCDD2-κ	LCDD3-λ
SORL1	-	-	-	SORL1	SORL1	SORL1	SORL1	SORL1	-
G-protein couple receptor	-	-	-	AGRL	AGRL	AGRL	AGRL	AGRL	AGRL
Ligand-gated ion channel/transient potential cation channel	-	-	-	TRPM	TRPM	TRPM	TRPM	TRPM	TRPM
Tyrosine-protein phosphatase	-	-	-	PTP	PTP	PTP	PTP	PTP	PTP
Extracellular matrix linker protein receptor	-	-	-	CAM	CAM	CAM	CAM	CAM	CAM

AGRL, G-protein couple receptor; AL, amyloidosis; CAM, Extracellular matrix linker protein receptor; DSTTP, ; GLC, glomerulopathic LC; LC, light chain; LCDD, LC deposition disease; MC, mesangial cell; PTP, Tyrosine-protein phosphatase; SORL1, sortilin-related receptor; TLC, tubulopathic LC; TRPM, Ligand-gated ion channel/transient potential cation channel. SORL1 was detected in 5 of 6 of the GLCs and the other receptors listed in the figure were detected in all 6 GLCs tested. Note that no cross-liked protein was detected when MCs were incubated in the same conditions with a TLC.

(normalized to total protein) with comparison of LCDD and AL-LCs is shown in Figure 1.

SORL1 Colocalization Is Specific to Both Types of GLCs in Caveolae on the Surface and Intracellularly in Lysosomes in MCs Incubated With AL-LCs Only

Using double fluorescence labeling techniques, SORL1 was colocalized with LCDD and AL-LCs (Figure 2a–d) on the surface of MCs and also inside of MCs in the latter (Figure 2: rows 1 and 2 from the top). Intracellular and extracellular domains of SORL1 were detected using ultrastructural immunogold labeling techniques (Figure 3). No colocalization was observed with TLCs (Figure 2: row 3 from the top). TLCs did not interact with MCs (Figure 2: row 4 from the top). Areas of colocalization were detected by yellow to white signals indicating the merging of green and red. Using transmission electron microscopy, SORL1 localized on the surface of MCs on caveolae (Figures 3 and 4) in both AL and LCDD tested LCs and in lysosomes when AL-LCs were tested (Figure 3a–d). Colocalization of GLCs with SORL1 at the surface caveolae on MCs using double ultrastructural immunolabeling with gold particles of different sizes (small 5–6 nm for LCs and large 15–16 nm for SORL1) was clearly demonstrated (Figure 5).

Completely transformed and hybrid MCs with partial (not complete) phenotypic transformation of MCs into a macrophage phenotype (Figure 6a–d) were observed with transmission electron microscopy only in MCs incubated with AL-LCs (not in those MCs incubated with T or LCDD-LCs).

CAV1 Staining of MCs Incubated With AL-LC was Markedly Increased Compared With MCs Incubated With No LC or With LCDD-LC

There was a marked increase in CAV1 staining in MCs incubated with AL-LCs with surface and marked intracellular staining identified. In contrast, staining for CAV1 was similar (not statistically significant) in MCs incubated with LCDD-LC and with no LCs (Figure 7). Approximately 70% new caveolae were identified on the surface of MCs incubated with GLCs, when compared with those incubated with TLCs or no LCs.

CAV1 Plays No Direct Role in Formation of Amyloid Fibrils

The role of CAV1 in amyloidogenesis was also explored in this study. CAV1 KO MCs incubated with amyloidogenic LCs showed no decrease in amyloid formation compared with AL-LC incubated with WT CAV1 MCs.

ECGC Cytotoxicity and Effect on MC Proliferation

ECGC was not cytotoxic to MCs at concentrations from 5 to 50 μM, but LDH release increased significantly compared with control at 100 μM, and cell number was significantly reduced at 100 μM but not at lower concentrations. At present, we do not have an explanation for the biological effect exerted by ECGC on MCs at 100

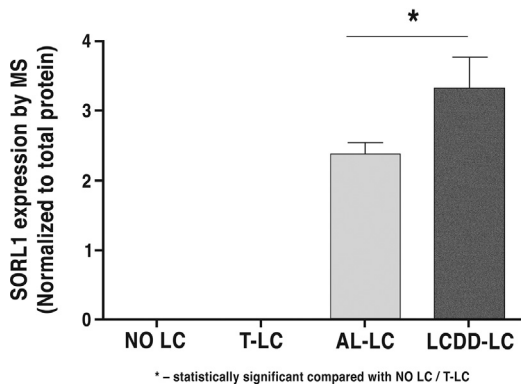

Figure 1. Mass spectroscopy analysis to evaluate the expression of SORL1 on MCs when incubated with GLCs (AL and LCDD-LCs), TLCs, and with no LC for 30 minutes and cross-linked. Note that intensity of expression of SORL1 on MCs was highest for LCDD-LC (more than for AL-LCs) and the degree of expression for both GLCs was statistically significant when compared with MCs incubated with TLCs and with no LCs. Data shown as the mean plus 1 SD of the results of 4 independent experiments. AL, amyloidosis; GLC, glomerulopathic LC; LC, light chain; LCDD, LC deposition disease; MC, mesangial cell; SORL1, sortilin-related receptor; TLC, tubulopathic LC.

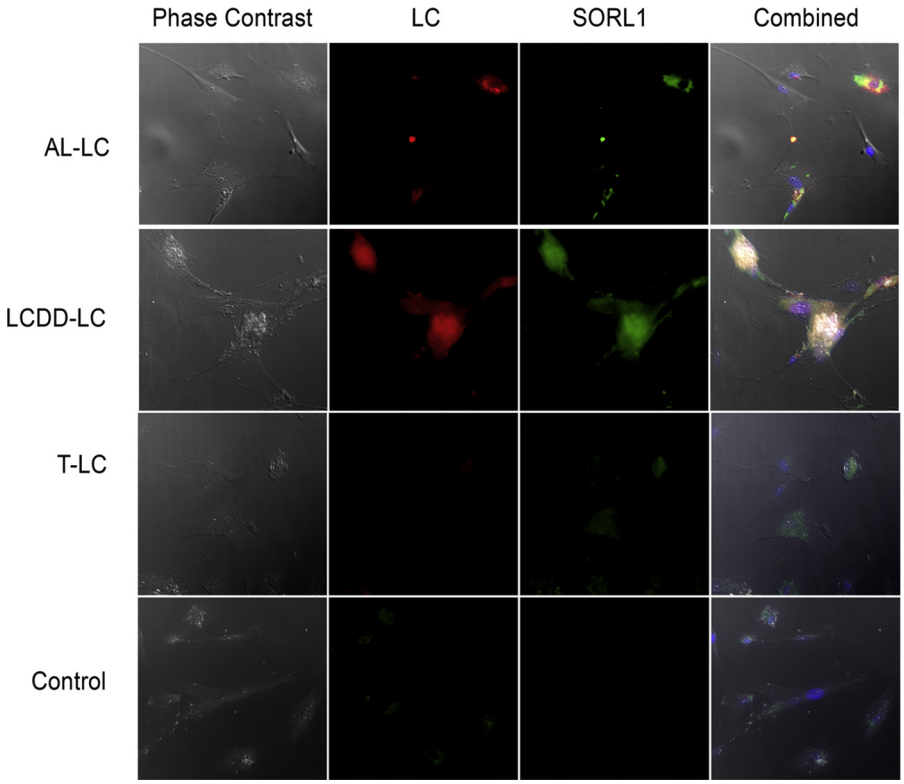

Figure 2. MCs incubated with G and TLCs and control (no LC) for 30 minutes. Immunofluorescence staining for SORL1-red and GLCs-green. Row 1: with AL-LCs-green; row 2: with LCDD-LCs; row 3 TLCs, and row 4: control. Column 1 shows phase contrast microscopy, column 2 fluorescence staining for pertinent light chain, column 3 staining for SORL1, and combined expression for both LCs and SORL1 in fourth column to assess for colocalization. All rows ×200. Note areas where both SORL1 and AL and LCDD-LCs colocalized (yellow to white areas) in the fourth column labeled combined. Note absence of labeling for TLCs for the LCs and rather subdued expression for SORL1 and in column labeled combined-labeling SORL1 only, similar to no LC panel with no colocalization. The findings clearly indicate that only GLCs interact with the SORL1 receptors on MCs. Note areas where LCs colocalize with SORL1 in activated MCs are only identified in activated (which appear rounded) MCs. Not all MCs are activated at the same time. Some MCs seen in the background (phase contrast) retain their normal shape and are not showing colocalization, as they are not interacting with LCs at the moment the photo was taken Representative image of 2 independent experiments. AL, amyloidosis; GLC, glomerulopathic LC; LC, light chain; LCDD, LC deposition disease; MC, mesangial cell; SORL1, sortilin-related receptor; TLC, tubulopathic LC.

μM. Studies in tumoral cell culture using EGCG at 100 μM have been performed and no toxicity was observed.[26] It cannot be excluded that the effect we observed in MCs reflects some idiosyncratic response of this cell type. Therefore, the concentration of 50 μM was not cytotoxic to MCs and did not significantly inhibit cell proliferation (Figure 8).

Interaction of GLs With MCs Modifies Compartmentalization of NF-κB and c-Fos, an Effect Reversed by EGCG

Western blot analysis of expression of NF-κB and c-Fos in MCs showed that in control situations and absence of GLCs, both proteins were almost exclusively expressed in the cytoplasm (Figure 9). However, incubation of MCs with either AL or LCDD- LCs shifted the NF-κB and c-Fos expression to the nucleus. The shifted effect of both GLCs was inhibited by ECGC in a concentration dependent manner, returning protein compartmentalization to control conditions at 50 μM EGCG. Of relevance, the effect of ECGC was more pronounced when AL rather than LCDD-LCs were used in the experiments (Figure 9). NF-κB and c-Fos compartmentalization changes induced by GLCs detected by Western blots were confirmed by immunofluorescence microscopy. In MC control conditions (negative control) and MCs incubated only with 50 μM EGCG (positive control) NF-κB was abundant in the cytoplasm. However, after MCs were incubated with AL or LCDD-LCs, NF-κB translocated to the nuclei. Co-incubation of MCs with GLCs and 50 μM ECGC revealed a significant decrease in nuclei and increased in the cytoplasm (almost to the same degree as in negative and positive control groups) in AL-LCs. In LCDD-LC co-incubation samples, NF-κB was mainly seen in cytoplasm with virtually no staining remaining in nuclei (Figure 10). On the other hand, similar to NF-κB, c-Fos was predominantly observed in the cytoplasm in the negative and positive control groups. However, after incubation with GLCs, c-Fos was mostly seen in nuclei and

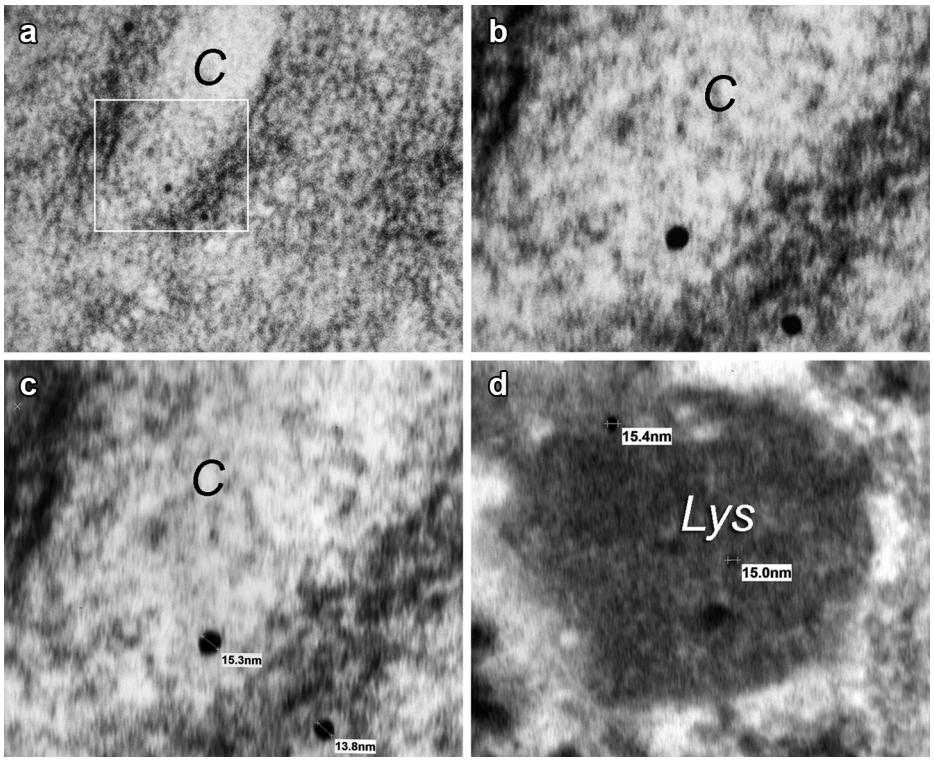

Figure 3. (a–d) Ultrastructural gold immunolabeling for SORL1. GLCs incubated with MCs for 30 minutes. Transmission electron microscopy. Uranyl acetate and lead citrate stain. Gold particles approximately 15 nm in diameter. (a) ×20,000, (b) ×25,500, (c) ×45,000, and (d) ×30,000. Note labeling of both extra and intracellular domains of SORL1 in (a–c) (gold particles) in caveolae (c). Outlined area in (a) is magnified in (b). Also note labeling of lysosomes (Lys) only for AL-LCs (d). No lysosomal labeling noted for LCDD-LCs. Representative images of 3 independent experiments. AL, amyloidosis; GLC, glomerulopathic LC; LC, light chain; LCDD, LC deposition disease; MC, mesangial cell; SORL1, sortilin-related receptor.

significantly decreased in the cytoplasm. When co-incubated with AL-LCs and ECGC, nuclear c-Fos was significantly decreased and mostly seen in the cytoplasm, similar as in the negative control. Co-incubation of LCDD-LCs with EGCG resulted in abundant NF-κB in the cytoplasm with only minimal amounts seen in nuclei (Figure 10). These results mirrored the Western blot results.

ECGC Decreases Amyloid Formation

EGCG pretreatment resulted in decreased amyloid formation (approximately 75% less amyloid) when amyloidogenic LCs were incubated with MCs for 72 hours, linked to inhibition of c-Fos signaling transferring from the MC cytoplasm to the nuclei.

c-Fos expression was abolished when CAV1 WT MCs were incubated with AL-LC but preserved when incubated with LCDD-LC (Figure 11). In contrast, c-Fos was reestablished when CAV1 KO MCs were incubated with AL-LC (Figure 11).

DISCUSSION

Our previous studies have demonstrated that both LCDD and AL-LCs interact with MCs through the same receptor, but its activation leads to divergent downstream MC/matrix alterations resulting in diametrically opposite changes in mesangial homeostasis.[18,27,28] In addition, we have previously demonstrated that GLCs interact with MCs in a dose- and time-dependent manner.[18] Importantly, it was also shown that although AL-LCs are avidly internalized into MCs for intracellular processing, the key interaction for the LCDD-LCs occurs at the MC surfaces. Despite the abundance of data strongly suggesting that a receptor-dependent mechanism plays a central role in the mesangial-centered pathobiological events derived from the interaction of GLCs with MC, the identity of such receptors has remained unknown,[18] until now. In this study, we provide evidence indicating that SORL1, a protein member VPS10P domain receptor gene family, is involved in the interactions with both AL-LCs and LCDD-LCs that take place at the membrane of MCs.

SORL1 was the LC's partner more frequently detected in several crosslinking experiments performed with both, LCDD-LCs and AL-LCs. This finding suggests that this protein is the receptor, or part of a membrane complex that functions as receptor for both types of GLCs in MCs. The evidence indicates that there are differences between these proteins with

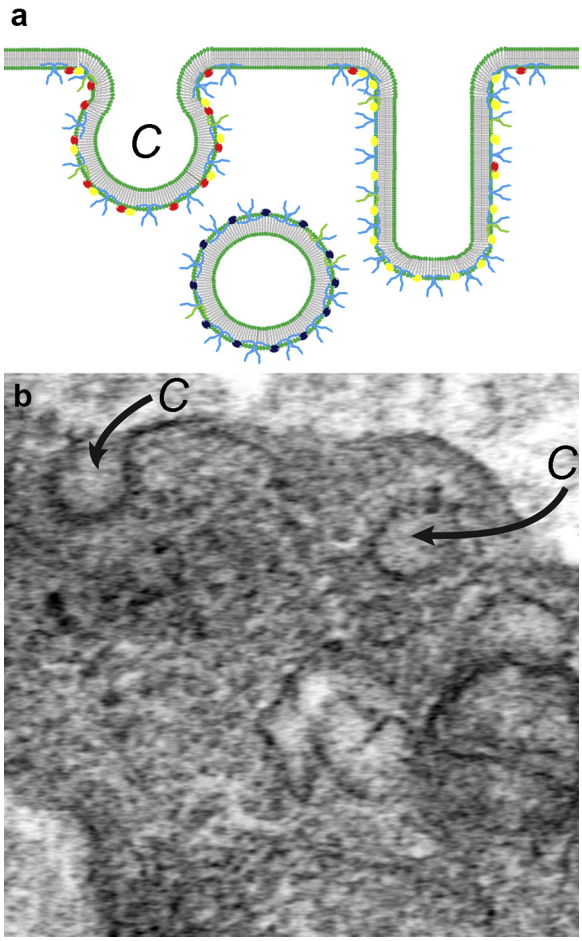

Figure 4. MCs incubated with GLCs for 30 minutes. (a) Caveolae, (c) diagrammatic representation and actual ultrastructural appearance in (b) ×20,000. Caveolae appear as cup- or flask-shaped structures at the cell surfaces. Caveolae increased dramatically when MCs were incubated with GLCs. Representative image of 5 independent experiments. Arrows point to caveolae formed in mesangial cell incubated with glomerulapathic light chains. GLC, glomerulopathic light chain; MC, mesangial cell.

respect to which intracellular signal pathway will be activated and which biological processes will be initiated once the LC binds to the membrane receptor. In contrast to AL-LCs, LCDD-LCs remain at the cell surface of the MCs, where they interact with SORL1 and CAV1 to impart message to the nuclei leading to activation of c-Fos. The consequence is the phenotypic transformation of the MC into myofibroblastic phenotype, with increase in the production of matrix proteins with abundant tenascin, packing in Golgi complex, and secretion into the extracellular space (Figure 12). This may explain why SORL1 is documented to be expressed more in LCDD than in AL-LCs incubated with GLCs (Figure 1). On the other hand, the interaction of AL-LC with SORL1 causes its internalization and routing to the endosomes, with which the recruitment of Rab proteins transport them to the mature lysosomal compartment, where AL-LCs are processed. The stringent conditions that characterize the lysosome promote the destabilization and misfolding of the LC and its assembly into amyloid fibrils, which are then extruded into the extracellular space.[29] We hypothesize that the amyloid aggregates produced inside the MCs from the internalized AL-LC monomers, once extruded into the extracellular space, can seed the amyloidogenesis of the soluble LC monomers, a hypothetical mechanism that could contribute to initiate, or at least bolster, AL deposition in kidney.

GLCs interact with the unique structures of MCs located at the cell membranes that have been characterized as caveolae where specific signaling, depending on the type of GLCs, are generated that alter MC and matrix homeostasis. GLCs (but not TLCs) induce the formation of caveolae at the surface of MCs[18] (Figure 4). In this study, we have shown that GLCs and SORL1 colocalize in caveolae at the MC surfaces (Figure 3).

We also demonstrate that SORL1 is uniquely expressed when GLCs interacted with MCs and not when TLCs were incubated with MCs or when MCs were incubated without LCs.[30] Remarkably, 5 of the 6 GLCs assayed in crosslinking experiments with MCs were found to be physically associated with SORL1. Reasons for the inability to identify a given receptor in one of the assayed GLCs are several, as perturbation of the receptor structure and/or ligand binding ability caused by conformational alterations that may occur depending on temperature variations associated with storage, and crosslinking conditions of the samples. The LC from the 1 patient with LCDD in whom SORL1 was not detected (Table 1) had been stored for more than 10 years (the longest of all GLCs tested) and exposed to unusual weather conditions during transportation from one laboratory to another. These facts likely account for the inability to detect SORL1 associated with this particular LC in the crosslinking experiment.

Taken together, our findings strongly suggest the interaction of GLCs with SORL1 when these proteins are incubated with MCs. To provide conclusive evidence of such interaction, in an ongoing study, additional experiments based on Forster Resonance Energy Transfer (FRET) are planned.

SORL1 gene encodes a transmembrane sorting receptor with intra- and extracellular domains that regulates trafficking of proteins in cells. Engagement of this receptor serves to direct the different types of GLCs to participate in unique signaling events and, in the case of AL-LCs, after endocytosis, to participate in the process of microvesicular movement inside the cells, resulting in the delivery of these LCs to the endolysosomal system and eventually, to mature lysosomes where crucial pathogenetic events occur (Figure 12).

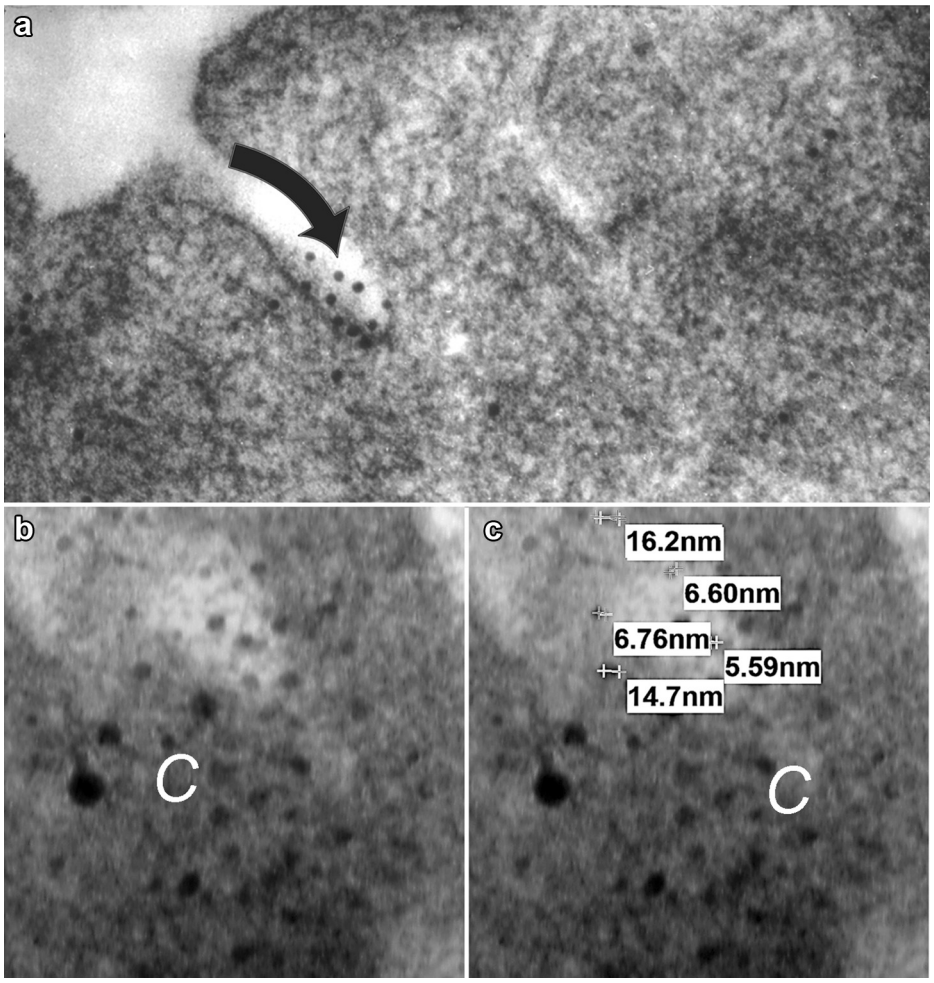

Figure 5. MCs incubated with (a) LCDD-LCs (κ) and (b) and (c) with AL-LCs (λ) for 30 minutes. Double ultrastructural immunogold labeling for SORL1, κ or λ LCs. LCs marked with 5- to 6-nm gold particles and SORL1 with 15- to 16-nm gold particles. Transmission electron microscopy. Uranyl acetate and lead citrate stain. Original magnifications: (a) ×22,500, (b) ×50,000, and (c) ×50,000. On (a), LCDD-κ LC interacting with surface caveola (c) on MC. Note on (b) and (c) colocalization on caveola at the surface of MCs for SORL1 (labeling intracellular and extracellular domains of SORL1, large gold particles) and amyloidogenic λ-LCs (small gold particles) on (b) and (c) with some LCs internalized. Representative images of 4 independent experiments. (a) was taken with permission from Herrera GA, Russell WJ, Isaac J, et al. Glomerulopathic light chain-mesangial cell interactions modulate in vitro extracellular matrix remodeling and reproduce mesangiopathic findings documented in vivo. *Ultrastruct Pathol*. 1999;23:107–126.11 AL, amyloidosis; LC, light chain; LCDD, LC deposition disease; MC, mesangial cell; SORL1, sortilin-related receptor.

SORL1 was previously identified to be present in large amounts in the brain and in less, but significant quantities, in the kidney, among other tissues, as demonstrated with mRNA expression studies (https://www.genecards.org/cgi-bin.carddisp.pl?gene=SORL1).[31] Furthermore, it was shown that SORLA is expressed in epithelial cells of the thick ascending limb of Henle's loop, where it plays a crucial role in the regulation of NKCC2 activation and for maintenance of renal ion balance.[31] However, there had been no specific cellular localization of SORL1 to the glomerulus before this study. SORL1 belongs to the Vps (vacuolar protein sorting) 10p-domain receptor family participating in the binding and transport of a variety of ligands such as neuropeptides and trophic factors.[32] Vps 10p-domain receptors serve as sorting factors that shuttle proteins from the cell surface to the endocytic and secretory cellular pathways and move hydrolases from the Golgi compartment to lysosomes, their place of action.[33]

SORL1 has been linked to receptors in psychiatric disorders, Alzheimer disease, and type 2 diabetes mellitus playing critical roles associated with neuronal functionality and metabolic control. Mutations of SORL1 have been associated with Alzheimer disease, a brain-centered disorder characterized by the presence of amyloid plaques.

Our data suggest that, in the glomerulus, SORL1 mediates MC activation by GLCs and in the case of AL-LCs, it mediates their internalization into MCs and delivery to lysosomes.

The early endosomes, also referred to as sorting endosomes, are involved in the sorting of receptors in the endocytic pathway.[34] Endocytosed proteins are

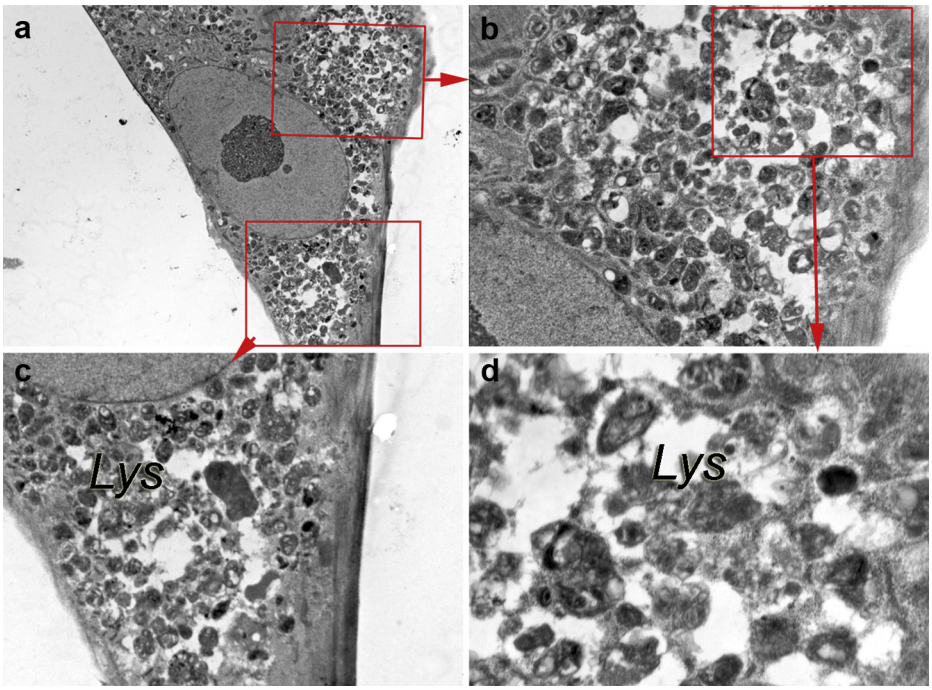

Figure 6. MCs incubated with λ AL-LC for 90 minutes. Transmission electron microscopy. Uranyl acetate and lead citrate. Areas shown in inserts marked in low-power magnification photos. (a) ×800, (b) ×2500, (c) ×6000, and (d) ×6000. Hybrid MC with almost complete macrophage phenotypic transformation. Outlined areas in (a) and (b) magnified as noted in (c) and (d). Abundance of lysosomes (*Lys*) in MCs (macrophage differentiation) with intracellular filaments with spindle densities (myofilaments) associated with attachment plaques at the periphery of the cell (indicating partial retention of smooth muscle differentiation), highlighted in Figure 5c. Some of the lysosomes (*Lys*) exhibit atypical shapes and partial loss of internal electron density (highlighted in Figure 5d) consistent with enzymatic activity related to LC processing. Representative images of 6 independent experiments. AL, amyloidosis; LC, light chain; MC, mesangial cell.

transported to the early endosomes after internalization from the plasma membrane. From the endosomes, cargo molecules are sorted to a variety of endocytic pathways, most importantly the endosomal/lysosomal pathway for degradation and recycling to the plasma membranes or to other endosomes located in the perinuclear endocytic recycling compartment.[35] In MCs, this intracellular trafficking pathway is carried out by Rab proteins.[18] Evidence of metabolic activity related to processing of internalized amyloid-producing LCs in the MC lysosomes is provided morphologically by the atypical shape of some of the lysosomes and partial loss of their electron density, as seen in Figure 5b (best appreciated in 5d) in an almost completely macrophage-transformed MC.

Caveolins are the signature proteins of specialized invaginations of the cell membranes with a diameter of 40 to 60 nm (caveolae) that function as structural elements and regulate signal transduction and other activities within the cells. Caveolae on the surface of MCs

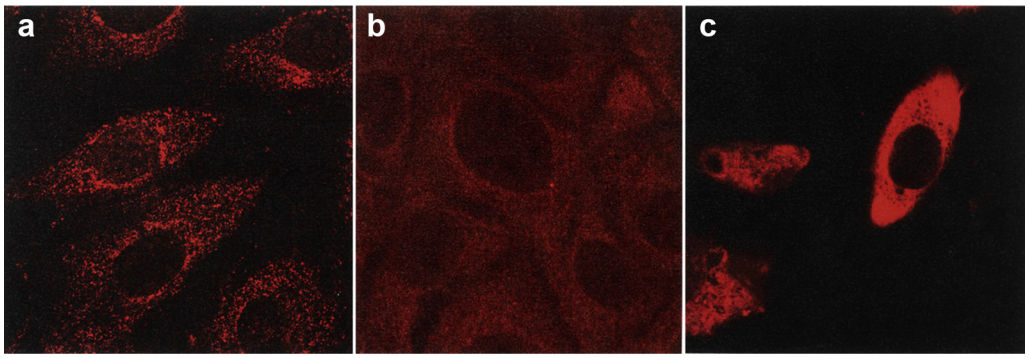

Figure 7. MCs incubated with AL, LCDD, and without LCs. Direct immunofluorescence for CAV1. Texas Red as marker. (a) No LC, (b) LCDD-LC, and (c) AL-LC. Magnification: (a) ×400, (b) ×400, and (c) ×400. Note significant increase in intracytoplasmic and surface staining for CAV1 in MCs incubated for AL-LC, as compared with those incubated with no LC or LCDD-LC (the latter two show similar staining). The images shown in this figure are representative of 6 independent experiments. AL, amyloidosis; LC, light chain; LCDD, LC deposition disease; MC, mesangial cell.

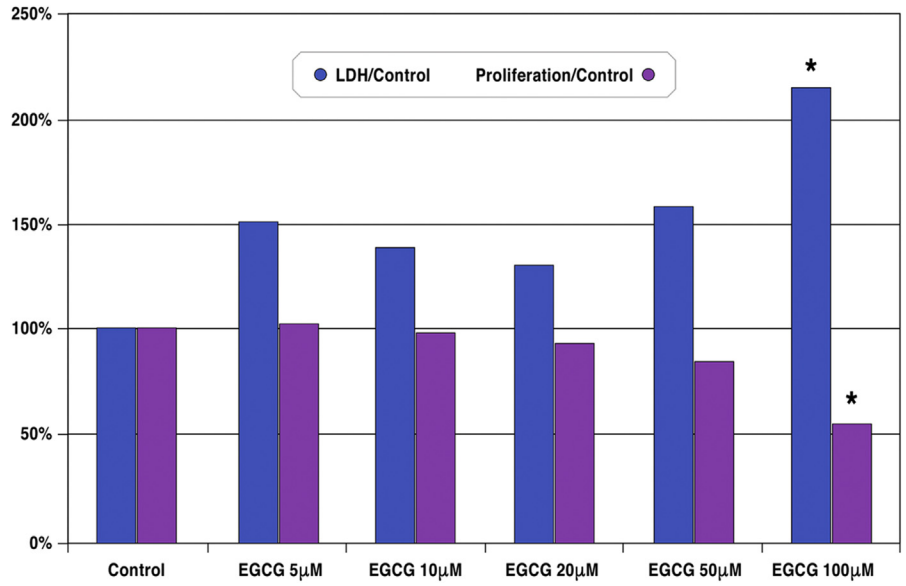

Figure 8. LDH concentration and MC numbers. MCs incubated with different concentrations of EGCG for 48 hours. EGCG in concentration up to 50 μM did not cause LDH release or MC proliferation. However, when EGCG was incubated with 100 μM, LDH release occurred and MC numbers were significantly reduced when compared with control. EGCG, epigallocatechin-3-gallate; LDH, lactic dehydrogenase; MC, mesangial cell.

participate in cellular signaling and exert significant, but not complete control of cellular signaling.[34,36–39] Processes can be stopped at different intracellular locations. Previous studies have shown that CAV1 is localized on the surface of MCs and the intensity of staining increases considerably when MCs are incubated with GLCs.[16,25] Caveolins have been hypothesized to maintain signaling proteins in an inactive form until a release "cue" is received, leading to translocation of signals such as those for c-Fos and NK-κB from cytoplasm to nuclei in MCs resulting in activation of certain cellular events. Based on the results

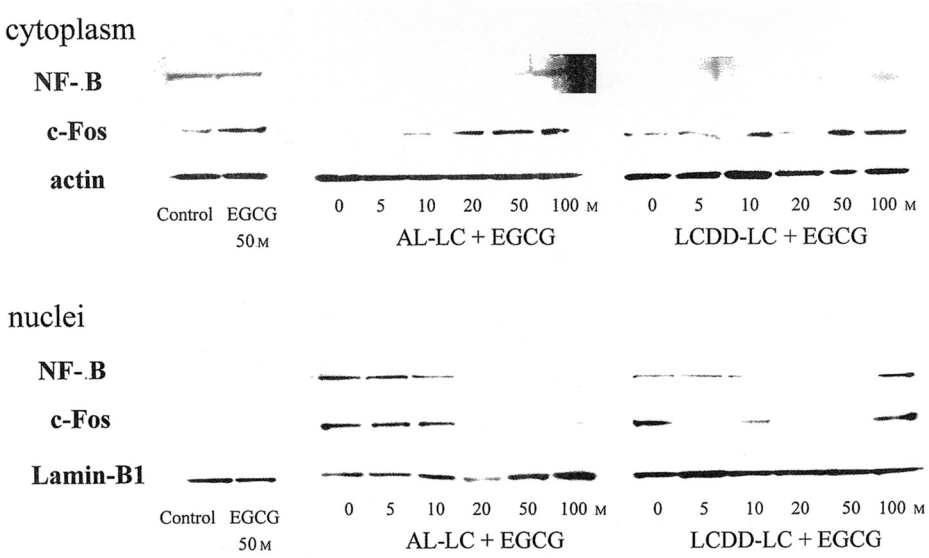

Figure 9. Western blot assays to evaluate the effect of incubation of MCs with EGCG at increasing concentration on expression of NF-κB and c-Fos in cytoplasmic (top half) and nuclear fractions (bottom half). In addition of the specified concentration of EGCG, MCs were incubated with an amyloidogenic (AL-) or LCDD-LC at 10 μg/ml. After incubation, MCs were labeled for NF-κB and c-Fos using immunofluorescence techniques demonstrating redistribution of signaling from cytoplasm to nuclei of MCs when incubated with GLCs. Normally NF-κB and c-Fos are located in the cytoplasm of MCs. When MCs are activated following incubation with GLCs (not with TLCs), both translocated from cytoplasm to nuclei. In contrast, when co-incubated with 50 μM of EGCG, this cytoplasmic to nuclear signal translocation did not occur. When co-incubated with several doses of EGCG, NF-κB and c-Fos expressions gradually decreased in the nuclear samples while it increased in the MC cytoplasm. AL, amyloidosis; EGCG, epigallocatechin-3-gallate; GLC, glomerulopathic LC; LC, light chain; LCDD, LC deposition disease; MC, mesangial cell; NF, nuclear factor; TLC, tubulopathic LC.

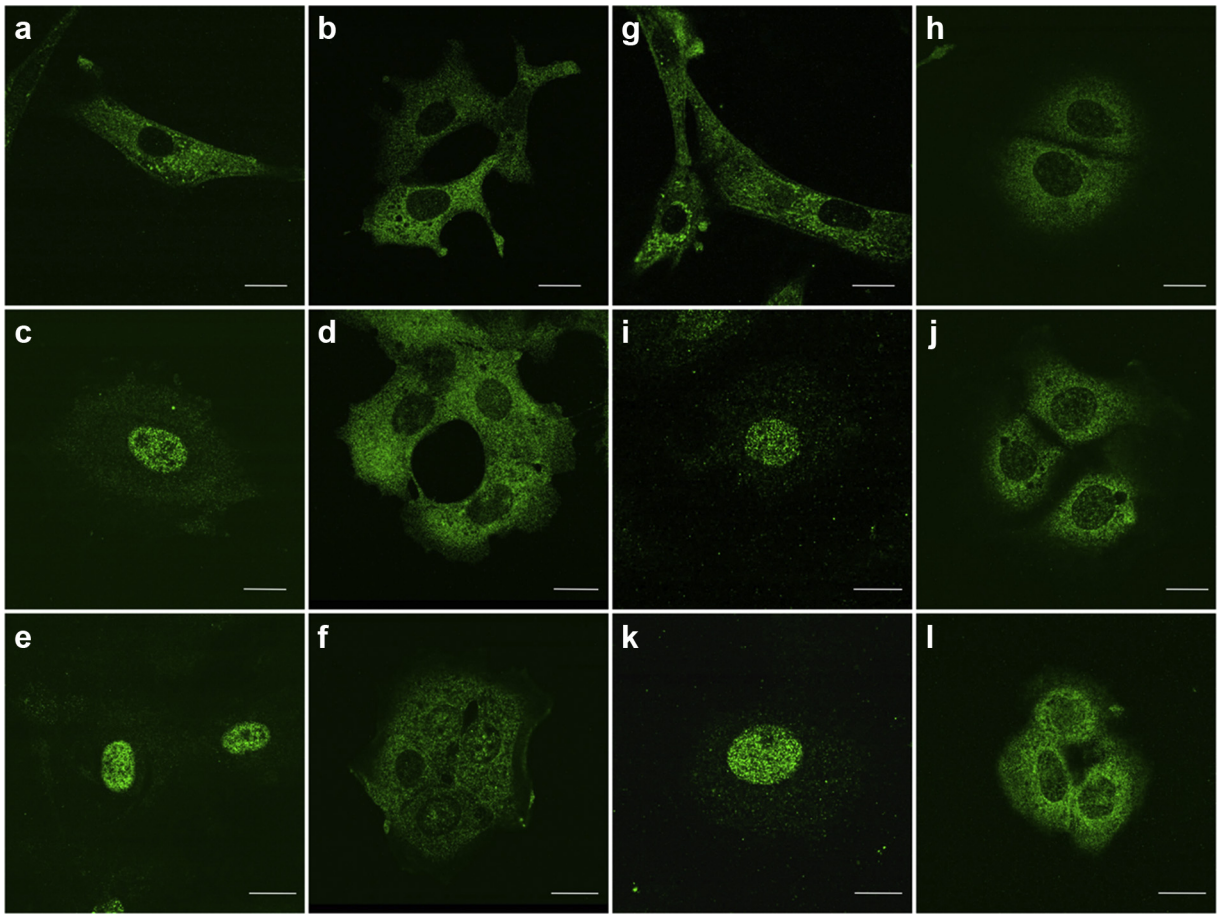

Figure 10. MCs incubated with 2 TLCs (TLC1 in a and b and TLC2 in g and h), and 4 GLCs (AL-LC1 in c and d, AL-LC2 in I and j, LCDD1 in e and f, and LCDD2 in k and l) at 10 μg/ml in absence (a, c, e, g, i, k) and in the presence of EGCG (b, d, f, h, j, l) at 50 μM for 48 hours. Immunofluorescence for NF-κB (a–f) and c-Fos (g–l). All images were obtained with magnification of ×500. Note inhibition of cytoplasmic to nuclear translocation of c-Fos signal when co-incubation of MCs with GLCs and EGCG was performed and, as a consequence, no phenotypic transformation of MCs as seen in Figure 5 occurs. AL, amyloidosis; EGCG, epigallocatechin-3-gallate; GLC, glomerulopathic LC; LC, light chain; LCDD, LC deposition disease; MC, mesangial cell; NF, nuclear factor; TLC, tubulopathic LC.

from the present study, we hypothesize that the interaction between GLCs and SORL1 likely represents such a "cue." These interactions are illustrated in the schematic representation in Figure 12.

Caveolins have been shown to play important roles in MC proliferation (platelet-derived growth factor-β driven) and matrix production (transforming growth factor-β controlled). Caveolins regulate platelet-derived growth factor-β, as receptors for this growth factor are also located in caveolae, and control transforming growth factor-β signaling, as transforming growth factor-β receptors are targeted to caveolae by interactions with Smad 7 and Smad ubiquitin regulatory factor (Smurf) protein.[40–48] Both platelet-derived growth factor-β and transforming growth factor-β are key growth factors in the pathogenesis of monoclonal light chain-related glomerulopathies.[11,12,21,49–51] When GLCs interact with MCs, c-Fos regulates MC proliferative activity (mediated through platelet-derived growth factor-β) and phenotypic transformation.[15]

Three caveolin isoforms have been identified: CAV1, caveolin- 2 (CAV2), and caveolin-3 (CAV3). Although CAV1 and CAV2 have been shown to be coexpressed in a wide range of tissues, including smooth muscle cells, CAV3 appears to be muscle-specific. CAV1 and CAV2 have also been shown to be present in lysosomes, especially in activated cells responding to various stimuli involved with exocytic and endocytic vesicular transport.[43] The 3 isoforms represent structural and scaffolding proteins that are key in the formation of caveolae and integral to their signaling functions.[52] In the glomerulus, caveolae have been detected on the surface of MCs in close proximity to pertinent receptors[18] that are activated by the binding of signaling molecules to a scaffolding domain of caveolin, which is composed of approximately 20 amino acids.[40,44]

The importance of CAV1 in GLCs-MC interactions is multifaceted. In previous study, using CAV1 KO MCs, it was demonstrated that in the LCDD-LC/MC *in vitro* signals were not transmitted from cell membranes to

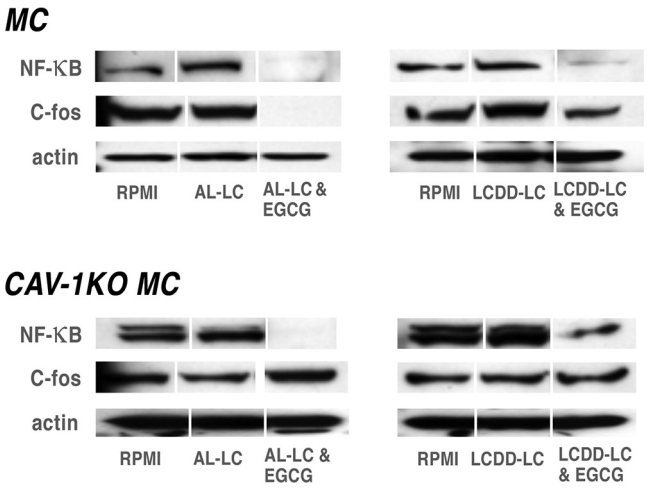

Figure 11. Western blot performed with cell extract of CAV1 KO and WT MCs incubated with AL or LCDD-LCs (10 μg/ml) for 60 minutes in the absence or presence of EGCG. Note that no signal for NF-κB nor c-Fos is detected in lane of WT CAV1 MCs incubated with AL-LCs in presence of ECGC. However, c-Fos but not NF-κB was clearly detected when WT cav-1 MCs were incubated with LCDD-LC in presence of ECGC. Incubation of cav-1 KO MC with AL-LC in presence of EGCG resulted in loss of expression of NF-κB, but not of c-Fos. AL, amyloidosis; EGCG, epigallocatechin-3-gallate; KO, knockout; LC, light chain; LCDD, LC deposition disease; MC, mesangial cell; NF, nuclear factor; WT, wild type.

effect MC phenotypic transformation into myofibroblasts, as occurs in CAV1 WT MCs. As a result, downstream extracellular matrix alterations resulting in expanded mesangium with increased matrix of abnormal composition did not occur.[20] In contrast, signal translocation for c-Fos and NF-κB was unaffected and similar amounts of amyloid fibril formation occurred when CAV1 KO MCs were incubated with amyloidogenic LCs. This could have resulted from compensation by the other caveolins or simply, CAV1 does not play a role in amyloid formation, regardless of its ability to participate in LC internalization into MCs. Also of note is the fact that migration of c-Fos and NF-κB occurs when both LCDD and AL-LCs interact with MCs. However, this signaling pathway is not as effective in AL-LCs as it is in LCDD-LCs. Regarding NF-κB, its role in MC pathobiology is still not completely understood, although it has been previously shown that it correlates with monocyte chemoattractant protein-1 production by MCs.[15]

The preceding data support 2 different signaling pathways at play when MCs interact with GLCs. The CAV1 pathway is crucial to elicit cellular changes that will eventually lead to the mesangial alterations that occur in LCDD that do not require internalization. In contrast, internalization into transformed MCs is a key component of the pathway in AL-Am that is controlled by c-Fos activation. EGCG controlling signaling step is

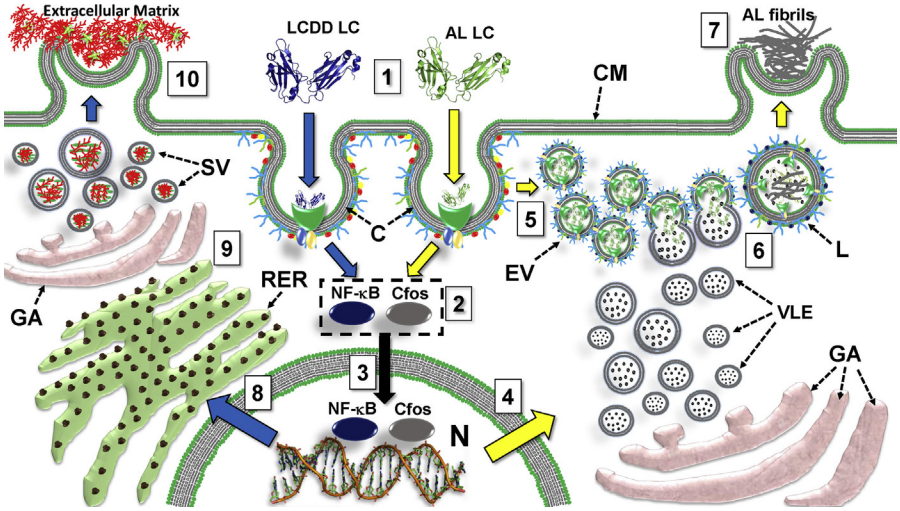

Figure 12. Schematic representation of signaling cascade in MCs when incubated with GLCs responsible for extracellular matrix alterations. Signaling cascade is shown with areas where inhibitors intervene. Inhibition of cascade can occur at the MC surface where caveolae are present but also at intracellular signaling cascade events. Note EGCG interferes directly with the translocation of c-Fos from cytoplasm to nuclei of MCs bypassing cav-1 at the MC surface. Initial interaction of GLCs and MCs leading to formation of caveolae (1). On initial interaction of AL-LCs at the MC surface with SORL1, NF-κB and c-Fos migrate from cytoplasm to nuclei of MCs (2,3) eliciting cellular activities (4). SORL1 mediated internalization of AL-LCs (5). Once AL-LCs are internalized they interact with endosomes (5), which with the recruitment of Rab proteins transport them to the mature lysosomal compartment (6) where AL-LCs are processed in the lysosomes (6). Amyloid fibrils are formed in lysosomes and extruded into the extracellular space (7). In contrast, LCDD-LCs interact with SORL1 at the cell surface and CAV1 (1) to impart message to MC nuclei leading to activation of c-Fos followed by MC phenotypic transformation into myofibroblastic phenotype (8) and engagement in the production of matrix proteins (9) with abundant tenascin, packing in Golgi complex, and secretion into the extracellular space (10). AL, amyloidosis; CM, cytoplasmic membrane; C, caveolae; EGCG, epigallocatechin-3-gallate; EV, endocytic vesicles; GA, Golgi apparatus; GLC, glomerulopathic LC; L, lysosome; LC, light chain; LCDD, LC deposition disease; MC, mesangial cell; N, nucleus; NF, nuclear factor; RER, rough endoplasmic reticulum; SORL1, sortilin-related receptor; SV, secretory vesicles; VLE, vesicles containing lysosomal enzymes.

mediated through c-Fos. In this study, we show that EGCG inhibits the activation of c-Fos directly impairing the translocation of c-Fos from cytoplasm to nuclei, resulting in inhibition of phenotypic transformation of MCs to a macrophage phenotype, a crucial event for amyloid formation to occur. Therefore, LC fibrillogenesis does not take place. In contrast, NF-κB (and not c-Fos) signaling is significantly decreased by EGCG in CAV1 KO MCs incubated with LCDD, suggesting that a different controlling mechanism is involved. These findings suggest that pharmacologic interventions in the signaling cascade can be potentially beneficial in patients with LC-associated glomerular damage.[53]

Membrane signaling systems perform numerous functions to impart information from the outside to MCs to react appropriately to various stimuli. A successful signaling system must discriminate among different signals to result in propagation of pertinent information and needs to be subject to modulation depending on circumstances, so that the signals generated do not overwhelm and injure cells. Membrane signaling systems are categorized into different groups: receptor tyrosine kinases, G protein-coupled systems, cell attachment/extracellular matrix receptors, ligand-gated ion channels, and others, including specific ones to a particular class of stimuli. Some of these systems are more generic, whereas others are more specific for the ligand-receptor interactions.[39] The pertinent transient receptors additionally identified in all 6 GLCs included G-protein-coupled, tyrosine-protein phosphatase and calcium ion channel receptors can be clearly understood in the setting of GLCs interacting with MCs (Table 1). G-protein-coupled receptors play an important role in caveolin signaling, whereas receptor type-tyrosine-protein phosphatase receptors are crucial generic elements in the signal transduction pathway.[40,54] Both of these transiently activated receptors are key for transmitting messages originating at the cell surface to the MCs to change their phenotypes and alter their functional activities resulting in profound changes in mesangial homeostasis, leading to the pathological alterations that occur. Finally, transient receptor potential cation channel subfamily M is an important calcium ion channel receptor,[55] which plays a pivotal role in activating MCs when exposed to GLCs, being the reorganization of the MC cytoskeleton and filopodia formation initiated by membrane interaction early morphological events of this process.[16] GLCs affect intracellular calcium homeostasis in MCs through alterations of the IP_3-dependent and independent pathways.[15]

Finally, we hypothesize that the ability of MCs to internalize AL-LC and route it to the lysosomal compartment, where its aggregation into amyloid occurs, plays a role in renal AL deposition.[56] As a nucleation-dependent process, LC amyloidogenesis is dramatically bolstered by the presence of preformed fibrils.[57] The LC amyloid aggregates extruded by MCs into the extracellular space, a finding previously reported by our group[29] (Figure 12), may act as recruitment points for soluble LC monomers, triggering the amyloid fibril elongation.[57] This hypothetical mechanism may contribute not only to initiate and/or bolster LC amyloidogenesis in kidney, also it may be a source of cytotoxic aggregates that cause MC damage by direct interaction with membrane components, as has been recently observed in cardiomyocytes.[29] A cell-dependent mechanism of seeding of LC amyloid aggregation may be relevant not only in kidney, because it has been recently shown that vascular smooth muscle cells also are capable of promoting AL formation by endocytosis and endolysosomal processing of LCs.[58] In conjunction, the finding of this study, as well as those previously reported by us and others, suggest that interfering the complex mechanism triggered by the interaction of GLC with its membrane receptor in MCs, in 1 or more of the several potential target points, may be a potential therapeutic strategy in both LCDD and AL-Am.[56] Ongoing studies in our laboratory pursue that goal.

CONCLUSIONS

This study demonstrates for the first time a new role of SORL1 as a key factor in the pathogenesis of glomerulopathies associated with monoclonal LCs. Signaling events at the cell surfaces (where SORL1 is also localized) mediated through caveolins control MC behavior and response to the monoclonal GLCs, but ECGC acts directly at the level of the mediator c-Fos, bypassing initial surface interactions where CAV1 is located.

Engagement of the SORL1 receptor serves to direct GLCs to different intracellular endolysosomal locations depending on their physicochemical characteristics where crucial pathobiological events take place. Figure 12 shows in a schematized fashion the interactions delineated in the article playing a role in the GLCs-MCs interactions with specific areas where inhibitors interfere with signaling cascades with potential therapeutic interventions.

The demonstration of the importance of SORL1 and interactions with other important cellular elements affecting mesangial pathobiology represents a significant advance in our understanding of how GLCs interact with MCs. It also provides a novel pharmacologic target that could be used to prevent or ameliorate the downstream events that take place when this receptor is activated by GLCs. The intricacies and

complexity of signaling and activation of cellular pathways initiated when GLCs interact with MCs are explored in this study, suggesting additional opportunities for therapeutic interventions. Furthermore, the divergent clinical and pathologic manifestations of AL-Am and LCDD are likely intimately related to the differences in the MC signaling events associated with these 2 disorders.

DISCLOSURES

All the authors declared no competing interests.

ACKNOWLEDGMENTS

This work was supported in part by a Senior Research Grant on Stem Cell from The Amyloidosis Foundation granted to GAH. We thank Adrian Hoff for his valuable contribution in the preparation of figures.

REFERENCES

1. Nakano T, Matsui M, Inoue I, et al. Free immunoglobulin light chain: its biology and implications in diseases. *Clin Chim Acta*. 2011;412:843–849.
2. Shapiro AL, Scharff MD, Maizel JV, et al. Synthesis of excess light chains of gamma globulin by rabbit lymph node cells. *Nature*. 1966;211:243–245.
3. Hopper JE, Papagiannes E. Evidence by radioimmunoassay that mitogen-activated human blood mononuclear cells secrete significant amounts of light chain Ig unassociated with heavy chain. *Cell Immunol*. 1986;101:122–131.
4. Mogensen CE, Solling. Studies on renal tubular protein reabsorption:partial and near complete inhibition by certain amino acids. *Scand J Clin Lab Invest*. 1977;37:477–486.
5. Wochner RD, Strober W, Waldmann TA. The role of the kidney in the catabolism of Bence Jones proteins and immunoglobulin fragments. *J Exp Med*. 1967;126:207–221.
6. Maack T. Renal handling of low molecular weight proteins. *Am J Med*. 1975;58:57–64.
7. Klassen RB, Allen PL, Batuman V, et al. Light chains are a ligand for megalin. *J Appl Physiol (1985)*. 2005;98:257–263.
8. Batuman V, Verroust PJ, Navar GL, et al. Myeloma light chains are ligands for cubilin (gp280). *Am J Physiol*. 1998;275:F246–F254.
9. Nielsen R, Christensen EI, Birn H. Megalin and cubilin in proximal tubule protein reabsorption:from experimental models to human disease. *Kidney Int*. 2016;89:58–67.
10. Li M, Balamuthusamy S, Simon EE, et al. Silencing megalin and cubilin genes inhibits myeloma light chain endocytosis and ameliorates toxicity in human renal proximal tubule epithelial cells. *Am J Physiol Renal Physiol*. 2008;295:F82–F90.
11. Herrera GA, Russell WJ, Isaac J, et al. Glomerulopathic light chain-mesangial cell interactions modulate in vitro extracellular matrix remodeling and reproduce mesangiopathic findings documented in vivo. *Ultrastruct Pathol*. 1999;23:107–126.
12. Keeling J, Herrera GA. The mesangium as a target for glomerulopathic light and heavy chains: pathogenic considerations in light and heavy chain-mediated glomerular damage. *Contrib Nephrol*. 2007;153:116–134.
13. Herrera GA. Renal lesions associated with plasma cell dyscrasias: practical approach to diagnosis, new concepts, and challenges. *Arch Pathol Lab Med*. 2009;133:249–267.
14. Lin J, Markowitz GS, Valeri AM, et al. Renal monoclonal immunoglobulin deposition disease:the disease spectrum. *J Am Soc Nephrol*. 2001;12:1482–1492.
15. Zhu L, Herrera GA, White CR, et al. Immunoglobulin light chain alters mesangial cell calcium homeostasis. *Am J Physiol*. 1997;272:F319–F324.
16. Russell WJ, Cardelli J, Harris E, et al. Monoclonal light chain–mesangial cell interactions:early signaling events and subsequent pathologic effects. *Lab Invest*. 2001;81:689–703.
17. Keeling J, Teng J, Herrera GA. AL-amyloidosis and light-chain deposition disease light chains induce divergent phenotypic transformations of human mesangial cells. *Lab Invest*. 2004;84:1322–1338.
18. Teng J, Russell WJ, Gu X, et al. Different types of glomerulopathic light chains interact with mesangial cells using a common receptor but exhibit different intracellular trafficking patterns. *Lab Invest*. 2004;84:440–451.
19. Teng J, Turbat-Herrera EA, Herrera GA. An animal model of glomerular light-chain-associated amyloidogenesis depicts the crucial role of lysosomes. *Kidney Int*. 2014;86:738–746.
20. Herrera GA, Turbat-Herrera EA, Teng J. Animal models of light chain deposition disease provide a better understanding of nodular glomerulosclerosis. *Nephron*. 2016;132:119–136.
21. Sirac C, Herrera GA, Sanders PW, et al. Animal models of monoclonal immunoglobulin-related renal diseases. *Nat Rev Nephrol*. 2018;14:246–264.
22. Keeling J, Herrera GA. An in vitro model of light chain deposition disease. *Kidney Int*. 2009;75:634–645.
23. Sanders PW, Herrera GA, Galla JH. Human Bence Jones protein toxicity in rat proximal tubule epithelium in vivo. *Kidney Int*. 1987;32:851–861.
24. Harper PA, Robinson JM, Hoover RL, et al. Improved methods for culturing rat glomerular cells. *Kidney Int*. 1984;26:875–880.
25. Herrera GA, Lott R. Colloidal gold labeling for diagnostic pathology. In: Hayat M, ed. *Colloidal Gold*. Vol. 3. New York: Academic Press; 1991:321–345.
26. Kim M, Murakami A, Kawabata K, et al. (−)-Epigallocatechin-3-gallate promotes pro-matrix metalloproteinase-7 production via activation of the JNK1/2 pathway in HT-29 human colorectal cancer cells. *Carcinogenesis*. 2005;26:1553–1562.
27. Keeling J, Herrera GA. Human matrix metalloproteinases: characteristics and pathologic role in altering mesangial homeostasis. *Microsc Res Tech*. 2008;71:371–379.
28. Teng J, Turbat-Herrera EA, Herrera GA. Role of translational research advancing the understanding of the pathogenesis of light chain-mediated glomerulopathies. *Pathol Int*. 2007;57:398–412.
29. Teng J, Turbat-Herrera EA, Herrera GA. Extrusion of amyloid fibrils to the extracellular space in experimental mesangial AL-amyloidosis: transmission and scanning electron microscopy studies and correlation with renal biopsy observations. *Ultrastruct Pathol*. 2014;38:104–115.
30. Herrera GA, Teng J, Shen, X, Turbat-Herrera EA, eds. Sortilin-related receptor (SORL-1) mediates glomerulopathic light

chain interactions with mesangial cells. [Abstract TH-OR055] *J Am Soc Nephrol*. 2018;29:16

31. Reiche J, Theilig F, Rafiqi FH, et al. SORLA/SORL1 functionally interacts with SPAK to control renal activation of Na(+)-K(+)-Cl(-) cotransporter 2. *Mol Cell Biol*. 2010;30:3027–3037.
32. Hermey G. The Vps10p-domain receptor family. *Cell Mol Life Sci*. 2009;66:2677–2689.
33. Januliene D, Manavalan A, Ovesen PL, et al. Hidden twins: SorCS neuroreceptors form stable dimers. *J Mol Biol*. 2017;429:2907–2917.
34. Ranganathan R. Biochemistry. Signaling across the cell membrane. *Science*. 2007;318:1253–1254.
35. Naslavsky N, Caplan S. The enigmatic endosome - sorting the ins and outs of endocytic trafficking. *J Cell Sci*. 2018;131: jcs216499.
36. Tamai O, Oka N, Kikuchi T, et al. Caveolae in mesangial cells and caveolin expression in mesangial proliferative glomerulonephritis. *Kidney Int*. 2001;59:471–480.
37. Parton RG. Cell biology. Life without caveolae. *Science*. 2001;293:2404–2405.
38. Williams TM, Lisanti MP. The caveolin proteins. *Genome Biol*. 2004;5:214.
39. Miller RT. The impact of molecular biology on understanding renal signal transduction. *Semin Nephrol*. 1992;12:516–523.
40. Couet J, Li S, Okamoto T, et al. Identification of peptide and protein ligands for the caveolin-scaffolding domain. Implications for the interaction of caveolin with caveolae-associated proteins. *J Biol Chem*. 1997;272:6525–6533.
41. Fridolfsson HN, Roth DM, Insel PA, et al. Regulation of intracellular signaling and function by caveolin. *FASEB J*. 2014;28:3823–3831.
42. Mercier I, Jasmin JF, Pavlides S, et al. Clinical and translational implications of the caveolin gene family: lessons from mouse models and human genetic disorders. *Lab Invest*. 2009;89:614–623.
43. Mundy DI, Li WP, Luby-Phelps K, et al. Caveolin targeting to late endosome/lysosomal membranes is induced by perturbations of lysosomal pH and cholesterol content. *Mol Biol Cell*. 2012;23:864–880.
44. Okamoto T, Schlegel A, Scherer PE, et al. Caveolins, a family of scaffolding proteins for organizing "preassembled signaling complexes" at the plasma membrane. *J Biol Chem*. 1998;273:5419–5422.
45. Liu Y, Lu S, Zhang Y, et al. Role of caveolae in high glucose and TGF-beta(1) induced fibronectin production in rat mesangial cells. *Int J Clin Exp Pathol*. 2014;7:8381–8390.
46. Razani B, Zhang XL, Bitzer M, et al. Caveolin-1 regulates transforming growth factor (TGF)-beta/SMAD signaling through an interaction with the TGF-beta type I receptor. *J Biol Chem*. 2001;276:6727–6738.
47. Sundberg C, Friman T, Hecht LE, et al. Two different PDGF beta-receptor cohorts in human pericytes mediate distinct biological endpoints. *Am J Pathol*. 2009;175:171–189.
48. Zhang GY, He B, Liao T, et al. Caveolin 1 inhibits transforming growth factor-beta1 activity via inhibition of Smad signaling by hypertrophic scar derived fibroblasts in vitro. *J Dermatol Sci*. 2011;62:128–131.
49. Herrera GA. Renal manifestations of plasma cell dyscrasias: an appraisal from the patients' bedside to the research laboratory. *Ann Diagn Pathol*. 2000;4:174–200.
50. Herrera GA, Shultz JJ, Soong SJ, et al. Growth factors in monoclonal light-chain–related renal diseases. *Hum Pathol*. 1994;25:883–892.
51. Zhu L, Herrera GA, Murphy-Ullrich JE, et al. Pathogenesis of glomerulosclerosis in light chain deposition disease. Role for transforming growth factor-beta. *Am J Pathol*. 1995;147:375–385.
52. Srivastav RK, Ansari TM, Prasad M, et al. Caveolins; An Assailant or An Ally of Various Cellular Disorders. *Drug Res (Stuttg)*. 2019;69:419–427.
53. Hunstein W. Epigallocathechin-3-gallate in AL amyloidosis: a new therapeutic option? *Blood*. 2007;110:2216.
54. Gilman AG. G proteins: transducers of receptor-generated signals. *Annu Rev Biochem*. 1987;56:615–649.
55. Hille B. *Ion channels of excitable membranes*. Third Edition, 3rd edn. Sunderland, MA: Sinauer Associates; 2001.
56. Herrera GA, Teng J, Turbat-Herrera EA, et al. Understanding Mesangial Pathobiology in AL-Amyloidosis and Monoclonal Ig Light Chain Deposition Disease. *Kidney Int Rep*. 2020;5: 1870–1893.
57. Marin-Argany M, Lin Y, Misra P, et al. Cell damage in light chain amyloidosis: fibril internalization, toxicity and cell-mediated seeding. *J Biol Chem*. 2016;291:19813–19825.
58. Vora M, Kevil CG, Herrera GA. Contribution of human smooth muscle cells to amyloid angiopathy in AL (light-chain) amyloidosis. *Ultrastruct Pathol*. 2017;41:358–368.